Cobalt(I) Pincer Complexes as Catalysts for CO_2 Hydrogenation to Formate

Wenzhi Yao,[a] Chance M. Boudreaux,[a] Megan M. Wysocki,[a] Md. Kausar Ahmed,[a] Fengrui Qu,[a] and Elizabeth T. Papish[a]*

[a] Department of Chemistry and Biochemistry, University of Alabama, Shelby Hall, Tuscaloosa, Alabama 35487, United States

* Corresponding Author

Email address:

etpapish@ua.edu

ABSTRACT

Carbon dioxide hydrogenation with base to generate formate salts can provide a means of storing hydrogen in an energy dense solid. The stored hydrogen can later be released upon acidification of the formate salts or formic acid can be used directly in fuel cells. However, this application requires catalytic CO_2 hydrogenation, which would ideally use an earth abundant metal as the catalyst. In this article, six new (CNC)$Co^{I}L_2$ pincer complexes were synthesized and fully characterized, including single crystal X-Ray diffraction analysis on four new complexes. These complexes contain an imidazole-based (**1_R**) N-heterocyclic carbene (NHC) ring or a benzimidazole based NHC ring (**2_R**) in the CNC pincer. The R group is para to N on the pyridine ring and been varied from electron withdrawing (CF_3) to donating (Me, OMe) substituents. The L type ligands have included CO and phosphine ligands (in **$^{PPh3}2$** and **$^{PMe3}2$**). Thus, two known Co complexes (**1**, **1_{OMe}**) and six new complexes (**1_{Me}**, **1_{CF3}**, **2**, **2_{OMe}**, **$^{PPh3}2$**, **$^{PMe3}2$**) were studied for the CO_2 hydrogenation reaction. In general, the unsubstituted CNC pincer complexes bearing two carbonyl ligands led to the highest activity. The best catalyst, **2**, remains active for over 16 h and produces a turnover number of 39,800 with 20 bars of 1:1 CO_2 / H_2 mixture at 60 °C.

TOC Graphic

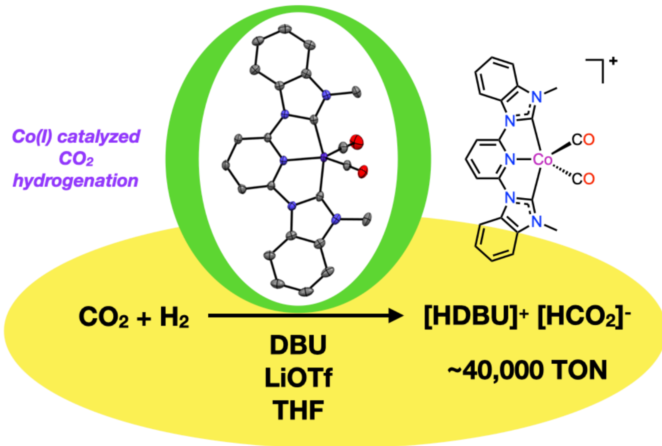

Keywords: Cobalt(I), hydrogenation, pincer ligands, carbon dioxide reduction, N-heterocyclic carbenes.

INTRODUCTION

The combustion of fossil fuels contributes to global warming due to increasing levels of CO_2 in the atmosphere. Carbon dioxide also represents an abundant carbon source which could be used for hydrogen storage.[1-2] Carbon dioxide hydrogenation in the presence of base (e.g. $NaHCO_3$) typically leads to formate salts (e.g. sodium formate) which can be used to store hydrogen in an energy dense solid.[3-6] (Scheme 1) These formate salts can be used as hydrogen storage materials with hydrogen and CO_2 release upon acidification of the compounds.[7]

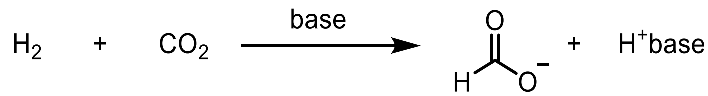

Scheme 1. CO_2 hydrogenation and to produce formate salts

The development of the homogeneous CO_2 hydrogenation has made significant progress in the past 30 years and has been summarized in several reviews.[5, 8-12] Several reports have used homogeneous catalysts based upon precious metals including Ir, Ru, Pd, and Rh.[13-25] For example, Nozaki's PNP iridium(III) catalyst (**Lit-1**, Figure 1) achieves 3.5×10^6 turnovers (TON) for CO_2 hydrogenation to form potassium formate.[13] However, iridium is one of the rarest elements in the Earth's crust. A more sustainable process can be envisioned by using earth abundant 3d transition elements for catalytic CO_2 hydrogenation and Mn,[26] Fe,[27] Co,[28-30] Ni[31] and Cu[32-33] complexes have been used as homogeneous catalysts for this reaction. Hazari and Bernskoetter reported that the (PNP)Fe(II) catalyst (**Lit-2**, Figure 1) hydrogenates CO_2 in the presence of the base 1,8-diazabicycloundec-7-ene (DBU) with nearly 60,000 TON due to rate acceleration from a Lewis acid (LiOTf) and metal-ligand cooperativity involving the nitrogen of the PNP ligand.[27] Similarly, the (PNP)Co(I) complex **Lit-3** (Figure 1) also takes advantage of the same factors (DBU and LiOTF) to produce 29,000 TON for CO_2 hydrogenation.[28]

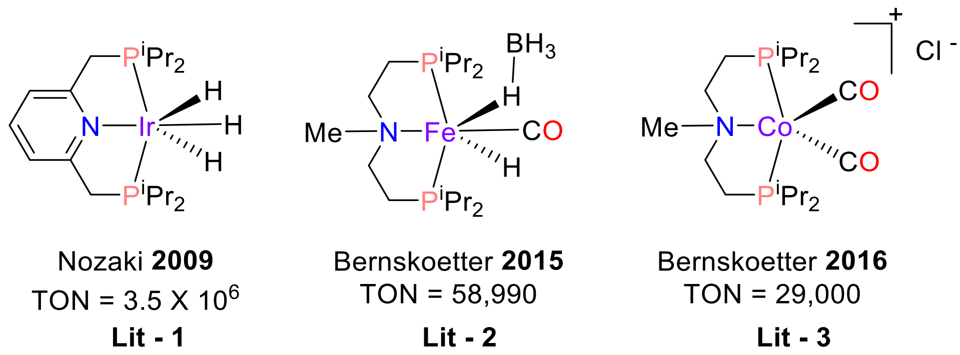

Figure 1. Previous examples of CO_2 hydrogenation.

We recently reported cobalt(I) and nickel (II) CNC pincer complexes that are active catalysts for photochemical CO_2 reduction via sacrificial electrons and protons to form CO and/or formate.[34-36] The CNC pincer ligand was derived from pyridine and N-heterocyclic carbene (NHC) donor groups wherein the pyridine electronic properties can be modulated by changing the substituent *para* to nitrogen.[37-38] We speculated that these cobalt(I) complexes may be viable catalysts for thermal CO_2 hydrogenation.

In this report, a series of Co(I) CNC pincer complexes (Figure 2) were synthesized and studied for CO_2 hydrogenation. The "**1**" series of compounds uses an imidazole derived NHC ring whereas the "**2**" series has a benzimidazole derived NHC ring in the CNC pincer. In our $^{\mathbf{L}}\mathbf{1}_{\mathbf{R}}$ and $^{\mathbf{L}}\mathbf{2}_{\mathbf{R}}$ nomenclature, L (when present) is the ligand that replaces a CO on cobalt(I) and R is the *para* substituent on the pyridine ring of the CNC pincer. Two of the complexes (**1** and $\mathbf{1}_{\mathbf{OMe}}$) were previously reported.[34] Six of the complexes are new including $\mathbf{1}_{\mathbf{Me}}$, $\mathbf{1}_{\mathbf{CF3}}$, **2**, $\mathbf{2}_{\mathbf{OMe}}$, $^{\mathbf{PPh3}}\mathbf{2}$, and $^{\mathbf{PMe3}}\mathbf{2}$. All eight complexes were studied herein for the CO_2 hydrogenation reaction to produce formate.

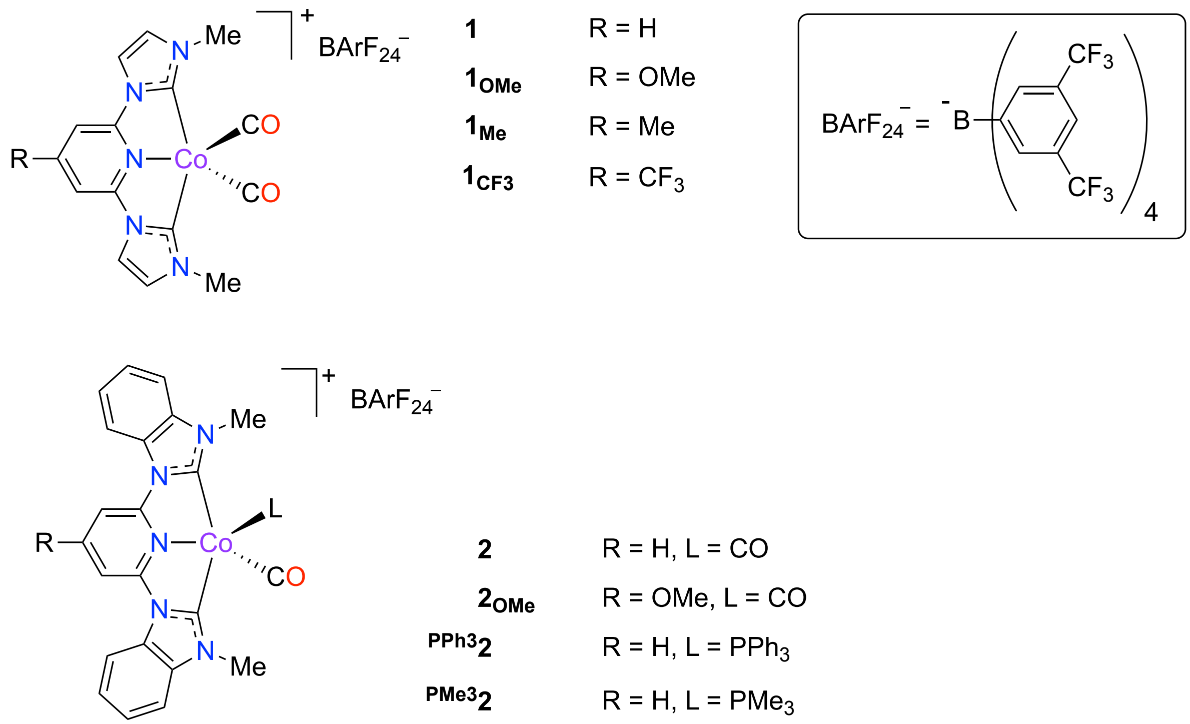

Figure 2. Structures of Co(I) CNC pincer catalysts used for CO_2 hydrogenation.

Results and Discussion

Synthesis. The synthesis of the cobalt(I) complexes (Figure 2) followed the procedures previously developed in the group.[34] Each preligand (**L1$_R$(HOTf)$_2$** and **L2$_R$(HOTf)$_2$**) was deprotonated with triethylamine in presence of $Co_2(CO)_8$ to make corresponding **1$_R$′** and **2$_R$′** complexes (Scheme 2). This disproportionation of $Co_2(CO)_8$ yielded the Co(I) CNC pincer complexes and a $[Co(CO)_4]^-$ anion (as the major product with some $[OTf]^-$ present) as observed in our prior publication and in the literature with other ligands.[34, 39-40] To avoid the presence of two Co sources during catalysis, a salt metathesis with sodium tetrakis(3,5-trifluoromethyl)phenyl)-borate ($NaBArF_{24}$) was performed to obtain pure **1$_R$** and **2$_R$** with the $BArF_{24}$ anion. Catalysts of type **1$_R$** and **2$_R$** were synthesized with a wide variety of R groups (R = H, OMe, Me, and CF_3 for **1$_R$** and R = H and

OMe for $\mathbf{2_R}$) to test both electron donating and withdrawing substituents. The yields of complexes $\mathbf{1_R}$ and $\mathbf{2_R}$ are reported in Scheme 2 and the supporting information and they range from 8 to 52% for two steps. With complex **2** (R = H), we also substituted one CO ligand with triphenyl phosphine ($^{\mathbf{PPh3}}\mathbf{2}$, >99% yield) or trimethyl phosphine ($^{\mathbf{PMe3}}\mathbf{2}$, >99% yield). These compounds were characterized by ^1H, ^{13}C, ^{19}F, and ^{31}P (for phosphine complexes) NMR, IR, and high res. MS or elemental analysis as described in the supporting information. Crystallographic data is reported for selected complexes as described below.

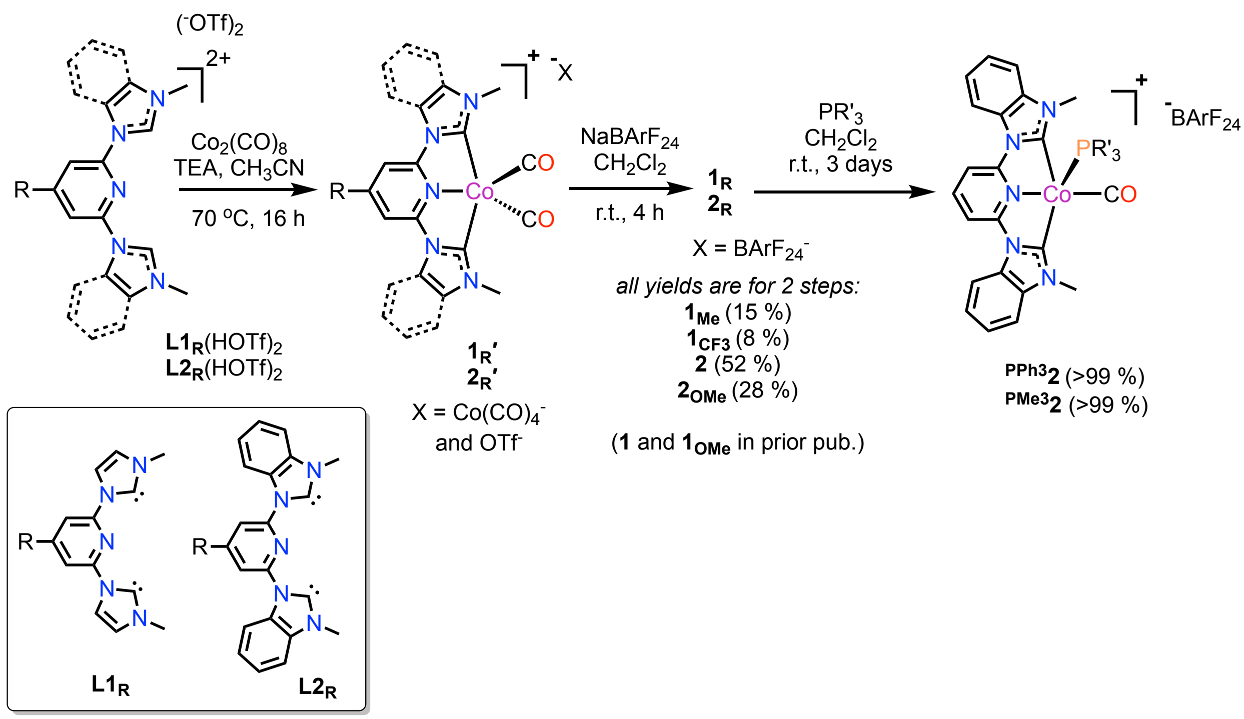

Scheme 2. Synthesis of cobalt(I) complexes used for CO_2 hydrogenation.

Single Crystal X-ray Diffraction. Crystals suitable for single crystal X-ray diffraction were obtained for $\mathbf{2_{OMe}}$ by slow evaporation of diethyl ether with a drop of acetonitrile. The other crystals were obtained by layering hexanes on top of either a concentrated solution of **2** or $^{\mathbf{PPh3}}\mathbf{2}$ in diethyl ether or a concentrated solution of ^{PMe3}**2** in dichloromethane. The structures of the complexes are shown in Figure 3 with a view of the primary coordination sphere to emphasize the change in geometry at the metal center upon phosphine coordination. The geometry index value τ_5 was also calculated and shown below each structure.[41] The parameter τ_5 ranges from 0 to 1, with the extreme values corresponding to a perfect square pyramid and a perfect trigonal bipyramid, respectively. As shown in Figure 3 and Table 1, all the dicarbonyl complexes have τ_5 values in the range around ~0.5 to 0.6 (including previously published values for **1** and $\mathbf{1_{OMe}}$). These distortions from trigonal bipyramid geometry are due to the chelate ring constraints, and do not represent distortions towards a square pyramid geometry since the carbonyl ligands are both equidistant from the plane of the pincer ligand. Compared to the dicarbonyl complex **2** (τ_5 = 0.559), its phosphine derivatives ^{PPh3}**2** (τ_5 = 0.284) and ^{PMe3}**2** (τ_5 = 0.222) are closer to a square pyramid geometry. This geometry change creates a free site *trans* to phosphine on the metal center.

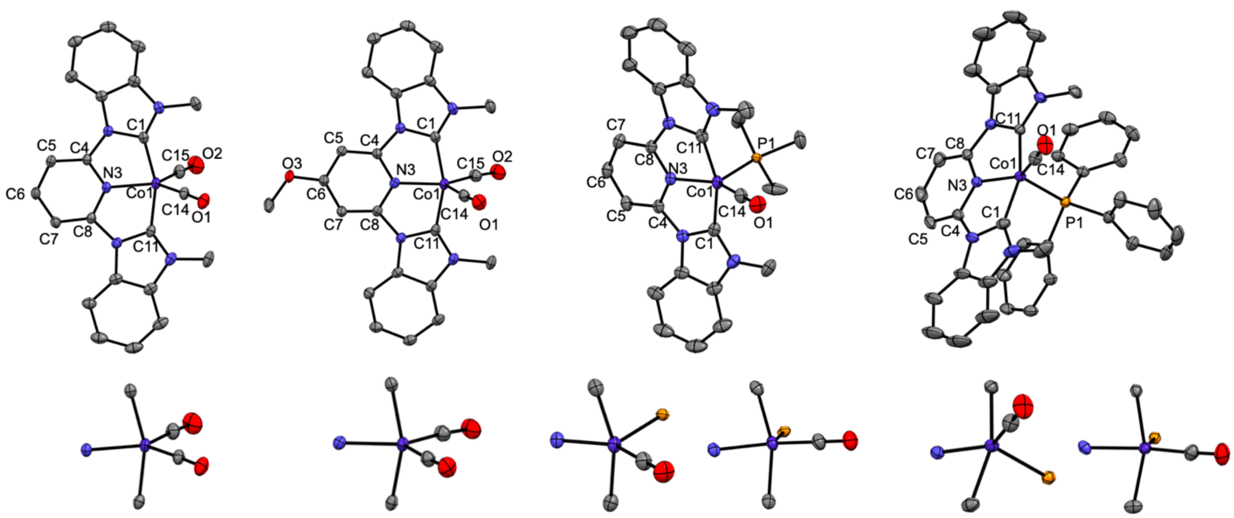

2 τ_5 = 0.559 | $\mathbf{2_{OMe}}$ τ_5 = 0.530 | ^{PMe3}**2** τ_5 = 0.222 | ^{PPh3}**2** τ_5 = 0.284

Figure 3. Molecular diagram of the new cobalt(I) complexes based on crystallographic data with hydrogen atoms and the $BArF_{24}$ anions removed for clarity. The cobalt first coordination sphere is

also shown for each complex along with the τ_5 parameter. Thermal ellipsoids are drawn at the 50% probability level.

As shown in Table 1, the Co-C(NHC) bond length decreased slightly from the imidazole derived complexes (**1_R**) to the benzimidazole complexes (**$^{L}2_R$**). The other distances around the metal center (Co-CO and Co-N) were similar across the series of dicarbonyl complexes. The substitution of one CO ligand for a phosphine results (in **$^{PMe3}2$** and **$^{PPh3}2$**) in a shortened Co-CO distance by ~0.04 Å which may be due to enhanced back bonding due to a more electron rich metal. The C6-O3 distance in **2^{OMe}** is 1.343(2) Å which shows that the methoxy group has partial double bond character due to resonance; similar bond distances have been noted in other methoxy substituted pincer complexes.[34, 37, 42-43]

Table 1. Selected bond lengths, angles, and τ_5 parameter for Co(I) complexes.[a] Complexes **1** and **1**$_{\mathbf{OMe}}$ were reported in a prior publication and are shown here for comparison.[34]

Designation	**1**	**1**$_{\mathbf{OMe}}$	**2**	**2**$_{\mathbf{OMe}}$	$^{\mathbf{PPh3}}$**2**	$^{\mathbf{PMe3}}$**2**
bond angles (°)						
N3−Co1−C$_{\mathbf{NHC\text{-}avg}}$	79.4(1)	79.3(1)	79.72(6)	79.67(7)	80.05(6)	80.25(6)
N3−Co1−C$_{\mathbf{CO\text{-}avg}}$	125.4(1)	125.2(1)	123.90(7)	124.33(8)	142.55(6)	146.14(6)
N3−Co1−P1					102.53(4)	104.09(8)
C14−Co1−L[b]	109.2(2)	109.7(1)	112.08(7)	111.3(1)	114.90(5)	109.76(9)
C1−Co1−C11	158.8(1)	158.6(1)	159.28(6)	159.28(8)	159.59(6)	159.43(6)
$\boldsymbol{\tau_5}$	0.548	0.545	0.559	0.530	0.284	0.222
bond lengths (Å)						
Co1−C$_{\mathbf{NHC\text{-}avg}}$	1.922(4)	1.914(3)	1.888(1)	1.894(2)	1.884(2)	1.876(1)
Co1−N3	1.916(3)	1.918(2)	1.908(1)	1.919(1)	1.902(1)	1.897(1)
Co1−C$_{\mathbf{CO\text{-}avg}}$	1.775(4)	1.775(4)	1.786(2)	1.769(2)	1.743(1)	1.743(2)
Co1−P1					2.2483(4)	2.236(3)
C$_{\mathbf{CO}}$**−O**$_{\mathbf{CO\text{-}avg}}$	1.145(6)	1.144(6)	1.138(2)	1.143(3)	1.153(1)	1.151(2)

[a]Averages are used when applicable. [b]L = C15 or P1 depending on respective metal bounded atom.

Vibrational Spectroscopy. Complexes **1** and **1_{OMe}** were previously studied by FTIR spectroscopy.[34] The dicarbonyl Co(I) cations have C_{2v} symmetry (Table 2 entries 1-6) and show A_1 symmetric carbonyl stretches of weak intensity between 2011 and 2034 cm^{-1} and B_2 asymmetric carbonyl stretches of strong intensity between 1958 and 1982 cm^{-1}. The phosphine substituted Co(I) cations (Table 2 entries 7 and 8) have C_s symmetry and only one carbonyl stretch is observed and is assigned as an A' vibrational mode. These phosphine complexes display a much lower CO stretch (at 1948-1949 cm^{-1}) than the dicarbonyl complexes (at 1958-2034 cm^{-1}) which reflects the electron donation from phosphine to the Co(I) center which allows for substantial backbonding to CO. For both type **1** (imidazole derived) and type **2** (benzimidazole derived) complexes, changing the R group on the pyridine ring from H to OMe (in **1** vs. **1_{OMe}** or **2** vs. **2_{OMe}**) increased the electron density at metal center for more back bonding to CO and decreased the carbonyl stretch by 10 – 21 cm^{-1}. It appears that Me and OMe are similarly electron donating, as **1_{Me}** and **1_{OMe}** display similar CO stretches. In contrast, changing the R group from H to the more electron withdrawing CF_3 has no influence on the A_1 stretch but it increased the B_2 mode by 9 cm^{-1} which is consistent with a less electron rich metal.

Table 2. Carbonyl stretching frequencies collected via FTIR-ATR for Co(I) complexes.

Entry	Complex	Carbonyl Frequencies [cm^{-1}]
1	**1**[a]	2025 (A_1), 1968 (B_2)
2	$\mathbf{1_{OMe}}$ [a]	2011 (A_1), 1958 (B_2)
3	$\mathbf{1_{Me}}$	2012 (A_1), 1960 (B_2)
4	$\mathbf{1_{CF3}}$	2025 (A_1), 1977 (B_2)
5	**2**	2034 (A_1), 1982 (B_2)
6	$\mathbf{2_{OMe}}$	2013 (A_1), 1962 (B_2)
7	$\mathbf{^{PPh3}2}$	1949 (A')
8	$\mathbf{^{PMe3}2}$	1948 (A')

[a] The values were previously reported.[34]

CO_2 hydrogenation. CO_2 hydrogenation reactions were studied by using a Parr reactor pressurized with 1:1 CO_2 and H_2. The reactions were run in tetrahydrofuran (THF) solution containing Co complex, lithium triflate (LiOTf) as a Lewis acid, and 1,8-diazabicyclo[5.4.0]undec-7-ene (DBU) as base to trap the product generated by the CO_2 hydrogenation (Scheme 3). While the role of DBU has been discussed and debated in the literature,[44] the current consensus is that DBU acts as a base and does not bind CO_2. In dry solvent, there is no evidence for a zwitterionic complex forming between DBU and CO_2.[45]

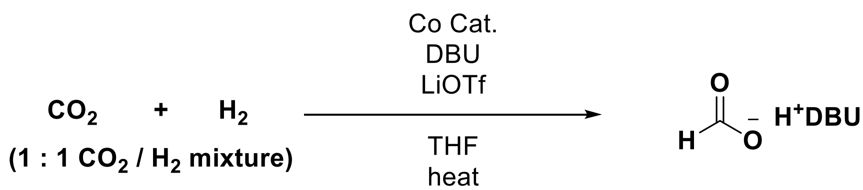

Scheme 3. CO_2 hydrogenation reaction catalyzed by Co(I) CNC pincer complex.

Several control experiments were run initially to determine the extent of background reaction in the absence of a catalyst (Table 3). The product ($HDBU^+$ HCO_2^-) is isolated in small amounts in the absence of cobalt or in the presence of a cobalt anion source (entries 1 and 2, respectively). Entry 2 shows that $NaCo(CO)_4$ produces less product than no cobalt catalyst, and thus shows no rate acceleration.

Table 3. Control experiments for CO_2 hydrogenation to form $[HDBU]^+[HCO_2]^-$.[a]

Entry	Catalyst	LiOTf	$[HDBU]^+[HCO_2]^-$
1	N/A	0.32 mmol	40(3) μmol
2	0.3 μmol of $NaCo(CO)_4$	0.32 mmol	32(5) μmol

[a]All experiments were done in triplicate. Conditions: Parr reactor was pressurized with 40 bars of CO_2 / H_2 mixture and 4.8 mmol of DBU and heated at 80 °C for 4 h after placing reaction mixture into the reactor in glovebox. Reaction mixture was prepared in 5 mL THF. See the Supporting Information for further details.

With control experiments completed, we tested eight catalysts for CO_2 hydrogenation in the presence of LiOTf and DBU (Table 4). These results show that with the imidazole derived NHC rings, catalyst **1** is most active with 11,000 TON. Surprisingly, any R group substitution within $\mathbf{1_R}$ catalysts gives a slight decrease in activity to ~3,000 to 4,000 TON for $\mathbf{1_{OMe}}$, $\mathbf{1_{Me}}$, and $\mathbf{1_{CF3}}$. We suggest that this trend is due to side reactions that lead to catalyst decomposition for $\mathbf{1_R}$ derivatives. A similar trend was observed between **2** and $\mathbf{2_{OMe}}$ (14,900 vs. 2,200 TON, respectively). Overall comparing **1** vs. **2** and $\mathbf{1_{OMe}}$ vs. $\mathbf{2_{OMe}}$, there is no clear trend with respect to benzimidazole vs. imidazole derived NHC rings, but **2** is the best catalyst of the group. Phosphine substitution for CO appears to decrease the TON values from 14,900 (**2**) to 12,000 ($\mathbf{^{PMe3}2}$) or 6,900 ($\mathbf{^{PPh3}2}$) (entries 8 and 9), but phosphine is not as detrimental as R group substitution on the pyridine ring. With the reasons for these trends being unclear, we proceeded with further experiments on **2** given that **2** is the best catalyst. Using these same conditions but stopping the reaction at different time points for analysis, it is apparent that the catalyst **2** is most active at the beginning of the reaction but it maintains activity for the full 16 hours (Table 5 and Figure 4).

Table 4. Catalyst activity for CO_2 hydrogenation.[a]

Entry	Complex	TON (×10^3)[b]
1	**1**	11(2)
2	$\mathbf{1_{OMe}}$	3.8(9)
3	$\mathbf{1_{Me}}$	2.74(7)
4	$\mathbf{1_{CF3}}$	4.2(6)
5	**2**	14.9(9)
6	$\mathbf{2_{OMe}}$	2.2(8)
7	$\mathbf{^{PMe3}2}$	12(2)
8	$\mathbf{^{PPh3}2}$	6.9(9)

[a]All experiments were done in triplicate or quadruplicate and were analyzed by ^{1}H NMR. Conditions: Parr reactor was pressurized with 40 bars of CO_2 / H_2 mixture and heated at 80 °C for 4 h after placing reaction mixture into the reactor in glovebox. Reaction mixture contains 6 μM Co complex, 0.384 M DBU, 64 mM LiOTf in THF solution. See the Supporting Information for further details. [b]Turnover number is calculated based on DMF internal standard added while preparing the NMR sample.

Table 5. Influence of reaction time.[a]

Entry	Time (h)	TON ($\times 10^3$)[b]
1	1	2.5(3)
2	2	5.3(1)
3	4	8.5(9)
4	8	11.0(3)
5	16	14(1)

[a]All experiments were done in triplicate or quadruplicate and were analyzed by ^1H NMR. Conditions: Parr reactor was pressurized with 40 bars of CO_2 / H_2 mixture and heated at 80 °C after placing reaction mixture into the reactor in glovebox. Reaction mixture contains 45.5 μM Co complex **2**, 1.92 M DBU, 64 mM LiOTf, and in THF solution. See the Supporting Information for further details. [b]Turnover number is calculated based on DMF internal standard added while preparing NMR sample.

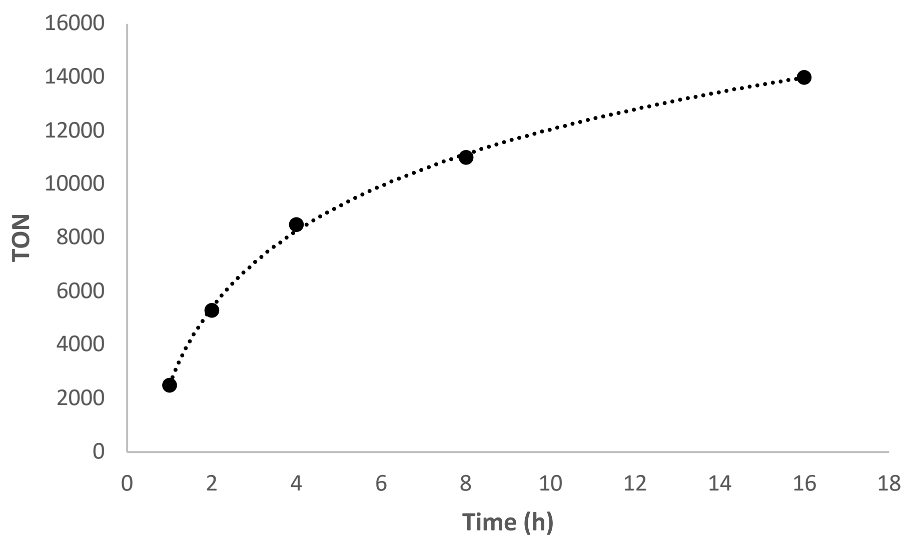

Figure 4. Turnover numbers with different reaction times for complex **2**.

Further studies on catalyst **2** were performed by varying the pressure and the temperature of the reaction (Table 6). Keeping the temperature constant at 80 °C and varying the pressure in entries 1-6 showed that 20 bar was the optimal pressure of 50/50 CO_2 and H_2. This may represent a compromise between having sufficient reactants, but too high a pressure may inhibit CO loss which would be necessary to generate a free site for catalysis. In entries 7-10, we used constant pressure and varied the temperature, which showed that 60 °C was optimal. This may represent a compromise between having sufficient activation energy, but avoiding high temperatures which may lead to decomposition. A full study of the initial rates as a function of temperature and measuring catalyst spectra before and after the reaction would be necessary to clarify this temperature dependence, however this is beyond the scope of the current work.

With these optimized conditions, the reaction was run on larger scale with 32.5 μM of complex **2**, 91.4 mM of LiOTf, and 2.7 M of DBU in 3.5 mL of THF solution under 20 bars of 1:1 CO_2 / H_2 mixture and heated at 60 °C for 16 h. The best TON observed for complex **2** under these conditions was $3.98(8) \times 10^4$.

Using the above information along with studies of similar catalysts in the literature,[26-28, 46] we can propose a mechanism for CO_2 hydrogenation in Scheme 4. The initial $[(CNC)Co(CO)_2]^+$ complex **2** is an 18 e- complex, which must lose a CO ligand to enable H_2 binding. The 16e- $[(CNC)Co(CO)]^+$ complex can bind H_2 to form a Co(I)-η^2-H_2 complex or a Co(III) dihydride, both of which have 18 electrons. Deprotonation with DBU then leads to a cobalt(I) hydride, [(CNC)Co (CO)H], which is poised to nucleophilically attack CO_2. The resulting formate complex can be O bound (most likely) or H bound. Formate dissociation then returns to the $[(CNC)Co(CO)]^+$ intermediate. The optimal rate involving intermediate pressure of CO_2/H_2 suggests that CO dissociation is required. Rate acceleration in the presence of Lewis acids has generally been attributed to Li^+ binding to formate and assisting in formate dissociation.[26-27, 46]

Table 6. The influence of pressure and temperature with catalyst **2**.[a] The optimal TON values were obtained with the conditions highlighted in red.

Entry	**Pressure (bar)**	**Temperature (°C)**	**TON ($\times 10^3$)[b]**
1	60	80	5.9(4)
2	40	80	8.5(9)
3	30	80	10.0(3)
4	20	80	22(1)
5	10	80	7.2(5)
6	5	80	6.5(5)
7	40	100	9.7(7)
8	40	60	21(3)
9	40	40	4.0(4)
10	40	22	4.1(4)

[a]All experiments were done in triplicate or quadruplicate and were analyzed by ^1H NMR. Conditions: Parr reactor was pressurized with CO_2 / H_2 mixture and heated for 4 h accordingly after placing reaction mixture into the reactor in glovebox. Reaction mixture contains 45.5 μM Co complex **2**, 1.92 M DBU, 64 mM LiOTf, in THF solution. See the Supporting Information for further details. [b]Turnover number is calculated based on DMF internal standard added while preparing NMR sample.

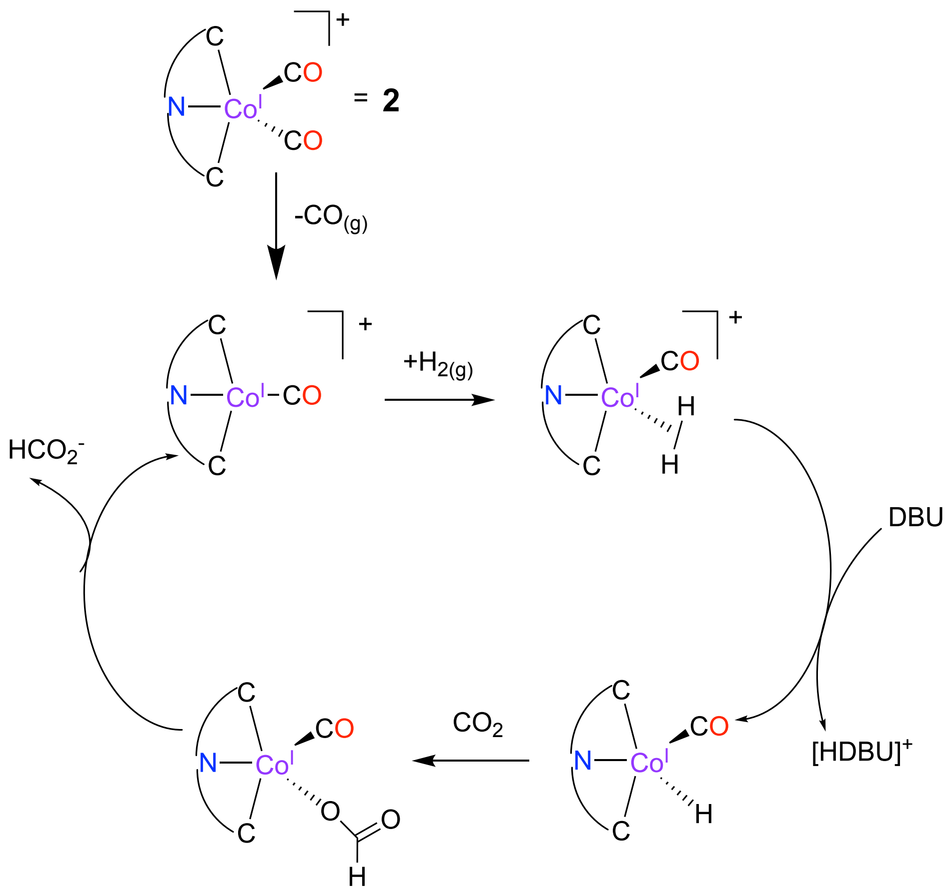

Scheme 4. A proposed mechanism using catalyst **2** for CO_2 hydrogenation.

Conclusions

Six new Co(I) CNC pincer complexes are reported with full characterization data including single crystal X-Ray diffraction on four complexes. A change in geometry from trigonal bipyramid to square pyramid is observed upon phosphine coordination. The vibrational spectra show the electronic influence of the R group on the pincer ring with electron donor groups (OMe, Me) resulting in CO stretch that is decreased due to increasing back-bonding from an electron rich Co(I) metal center. A similar influence is observed by coordination of an electron donating phosphine ligand. Eight complexes (six new and two previously reported) have been used as catalysts for CO_2 hydrogenation with DBU as the base and LiOTf as a Lewis Acid. Herein, the three most active catalysts (all with TON >10,000) are **2**, $^{\mathbf{PMe3}}$**2**, and **1** in order of decreasing activity (Table 4). It appears that R groups on the pincer ring which are either electron donating or withdrawing tend to decrease catalytic activity which may relate to catalyst decomposition pathways. Catalyst **2** was studied further, and it appears that moderate temperature (60 °C) and pressure (20 bar of 1:1 CO_2: H_2) results in higher catalytic activity. This may relate to key steps in the catalytic cycle involving CO ligand loss and CO_2 or H_2 coordination, which are thus favored by intermediate pressures. Likewise, faster rates at intermediate temperatures may relate to having sufficient activation energy but avoiding decomposition pathways. Using these optimized conditions, nearly 40,000 TON is achieved which surpasses other studies with Co(I) catalysts.[28] Future studies will aim to study this mechanism further by the method of initial rates with each catalyst.

AUTHOR INFORMATION

Corresponding Authors:
*E-mail: etpapish@ua.edu (E.T.P.).

ORCID

Wenzhi Yao 0000-0002-4874-0169
Chance M. Boudreaux 0000-0003-1322-9878
Fengrui Qu 0000-0002-9975-2573
Elizabeth T. Papish: 0000-0002-7937-8019

ASSOCIATED CONTENT

Supporting Information

The Supporting Information is available free of charge on the ACS Publications website at DOI: xxxx.

Experimental details on synthesis and characterization, single crystal X-ray diffraction, and catalysis (PDF)

Crystallographic information (XYZ)

ACKNOWLEDGMENT

The authors thank the NSF (CHE-1800214 and 2102416) for funding this research. We thank NSF CHE MRI 1828078 and UA for the purchase of the SC XRD instrument. We thank NSF CHE MRI 1919906 and UA for the purchase of an NMR spectrometer. We thank Dr. Ken Belmore for assistance with the NMR experiments. CMB thanks GAANN and AL EPSCoR for partial support.

CONFLICT OF INTEREST STATEMENT

The authors declare no conflict of interest.

References

1. Navarro, R. M.; Peña, M. A.; Fierro, J. L. G., Hydrogen Production Reactions from Carbon Feedstocks: Fossil Fuels and Biomass. *Chem. Rev.* **2007,** *107*, 3952-3991.
2. Eberle, U.; Felderhoff, M.; Schüth, F., Chemical and Physical Solutions for Hydrogen Storage. *Angew. Chem. Int. Ed.* **2009,** *48*, 6608-6630.
3. Filonenko, G. A.; Smykowski, D.; Szyja, B. M.; Li, G.; Szczygieł, J.; Hensen, E. J. M.; Pidko, E. A., Catalytic Hydrogenation of CO2 to Formates by a Lutidine-Derived Ru–CNC Pincer Complex: Theoretical Insight into the Unrealized Potential. *ACS Catal.* **2015,** *5*, 1145-1154.
4. Sordakis, K.; Dalebrook, A. F.; Laurenczy, G., A Viable Hydrogen Storage and Release System Based on Cesium Formate and Bicarbonate Salts: Mechanistic Insights into the Hydrogen Release Step. *ChemCatChem* **2015,** *7*, 2332-2339.
5. Wang, W.-H.; Himeda, Y.; Muckerman, J. T.; Manbeck, G. F.; Fujita, E., CO2 Hydrogenation to Formate and Methanol as an Alternative to Photo- and Electrochemical CO2 Reduction. *Chem. Rev.* **2015,** *115*, 12936-12973.
6. Liu, Q.; Wu, L.; Gülak, S.; Rockstroh, N.; Jackstell, R.; Beller, M., Towards a Sustainable Synthesis of Formate Salts: Combined Catalytic Methanol Dehydrogenation and Bicarbonate Hydrogenation. *Angew. Chem. Int. Ed.* **2014,** *53*, 7085-7088.
7. Siek, S.; Burks, D. B.; Gerlach, D. L.; Liang, G.; Tesh, J. M.; Thompson, C. R.; Qu, F.; Shankwitz, J. E.; Vasquez, R. M.; Chambers, N. S.; Szulczewski, G. J.; Grotjahn, D. B.; Webster, C. E.; Papish, E. T., Iridium and Ruthenium Complexes of NHC and Pyridinol Derived Chelates as Catalysts for Aqueous Carbon Dioxide Hydrogenation and Formic Acid Dehydrogenation: The Role of the Alkali Metal. *Organometallics* **2017,** *36*, 1091-1106.
8. Jessop, P. G.; Ikariya, T.; Noyori, R., Homogeneous Hydrogenation of Carbon Dioxide. *Chem. Rev.* **1995,** *95*, 259-272.
9. Jessop, P. G.; Joó, F.; Tai, C.-C., Recent advances in the homogeneous hydrogenation of carbon dioxide. *Coord. Chem. Rev.* **2004,** *248*, 2425-2442.
10. Leitner, W., Carbon Dioxide as a Raw Material: The Synthesis of Formic Acid and Its Derivatives from CO2. *Angew. Chem., Int. Ed.* **1995,** *34*, 2207-2221.
11. Wang, W.; Wang, S.; Ma, X.; Gong, J., Recent advances in catalytic hydrogenation of carbon dioxide. *Chem. Soc. Rev.* **2011,** *40*, 3703-3727.
12. Siegel, R. E.; Pattanayak, S.; Berben, L. A., Reactive Capture of CO2: Opportunities and Challenges. *ACS Catal.* **2023,** *13*, 766-784.
13. Tanaka, R.; Yamashita, M.; Nozaki, K., Catalytic Hydrogenation of Carbon Dioxide Using Ir(III)−Pincer Complexes. *J. Am. Chem. Soc.* **2009,** *131*, 14168-14169.
14. Schmeier, T. J.; Dobereiner, G. E.; Crabtree, R. H.; Hazari, N., Secondary Coordination Sphere Interactions Facilitate the Insertion Step in an Iridium(III) CO2 Reduction Catalyst. *J. Am. Chem. Soc.* **2011,** *133*, 9274-9277.
15. Munshi, P.; Main, A. D.; Linehan, J. C.; Tai, C.-C.; Jessop, P. G., Hydrogenation of Carbon Dioxide Catalyzed by Ruthenium Trimethylphosphine Complexes: The Accelerating Effect of Certain Alcohols and Amines. *J. Am. Chem. Soc.* **2002,** *124*, 7963-7971.
16. Tanaka, R.; Yamashita, M.; Chung, L. W.; Morokuma, K.; Nozaki, K., Mechanistic Studies on the Reversible Hydrogenation of Carbon Dioxide Catalyzed by an Ir-PNP Complex. *Organometallics* **2011,** *30*, 6742-6750.
17. Hutschka, F.; Dedieu, A.; Eichberger, M.; Fornika, R.; Leitner, W., Mechanistic Aspects of the Rhodium-Catalyzed Hydrogenation of CO2 to Formic AcidA Theoretical and Kinetic Study†,‖. *J. Am. Chem. Soc.* **1997,** *119*, 4432-4443.
18. Ocansey, E.; Darkwa, J.; Makhubela, B. C. E., Iridium and Palladium CO2 Hydrogenation in Water by Catalyst Precursors with Electron-Rich Tetrazole Ligands. *Organometallics* **2020,** *39*, 3088-3098.

19. Inoue, Y.; Izumida, H.; Sasaki, Y.; Hashimoto, H., Catalytic fixation of carbon dioxide to formic acid by transition-metal complexes under mild conditions. *Chem. Lett.* **1976,** *5*, 863-864.
20. Jessop, P. G.; Ikariya, T.; Noyori, R., Homogeneous catalytic hydrogenation of supercritical carbon dioxide. *Nature* **1994,** *368*, 231-233.
21. Huff, C. A.; Kampf, J. W.; Sanford, M. S., Role of a Noninnocent Pincer Ligand in the Activation of CO2 at (PNN)Ru(H)(CO). *Organometallics* **2012,** *31*, 4643-4645.
22. Vogt, M.; Gargir, M.; Iron, M. A.; Diskin-Posner, Y.; Ben-David, Y.; Milstein, D., A New Mode of Activation of CO2 by Metal-Ligand Cooperation with Reversible C-C and M-O Bond Formation at Ambient Temperature. *Chem. - Eur. J.* **2012,** *18*, 9194-9197, S9194/1-S9194/37.
23. Sanz, S.; Benítez, M.; Peris, E., A New Approach to the Reduction of Carbon Dioxide: CO 2Reduction to Formate by Transfer Hydrogenation in iPrOH. *Organometallics* **2010,** *29*, 275-277.
24. Himeda, Y.; Onozawa-Komatsuzaki, N.; Sugihara, H.; Kasuga, K., Simultaneous Tuning of Activity and Water Solubility of Complex Catalysts by Acid−Base Equilibrium of Ligands for Conversion of Carbon Dioxide. *Organometallics* **2007,** *26*, 702-712.
25. Himeda, Y.; Miyazawa, S.; Hirose, T., Interconversion between Formic Acid and H2/CO2 using Rhodium and Ruthenium Catalysts for CO2 Fixation and H2 Storage. *ChemSusChem* **2011,** *4*, 487-493.
26. Bertini, F.; Glatz, M.; Gorgas, N.; Stöger, B.; Peruzzini, M.; Veiros, L. F.; Kirchner, K.; Gonsalvi, L., Carbon dioxide hydrogenation catalysed by well-defined Mn(i) PNP pincer hydride complexes. *Chem. Sci.* **2017,** *8*, 5024-5029.
27. Zhang, Y.; MacIntosh, A. D.; Wong, J. L.; Bielinski, E. A.; Williard, P. G.; Mercado, B. Q.; Hazari, N.; Bernskoetter, W. H., Iron catalyzed CO2 hydrogenation to formate enhanced by Lewis acid co-catalysts. *Chem. Sci.* **2015,** *6*, 4291-4299.
28. Spentzos, A. Z.; Barnes, C. L.; Bernskoetter, W. H., Effective Pincer Cobalt Precatalysts for Lewis Acid Assisted CO 2Hydrogenation. *Inorg. Chem.* **2016,** *55*, 8225–8233.
29. Burgess, S. A.; Grubel, K.; Appel, A. M.; Wiedner, E. S.; Linehan, J. C., Hydrogenation of CO2 at Room Temperature and Low Pressure with a Cobalt Tetraphosphine Catalyst. *Inorg. Chem.* **2017,** *56*, 8580-8589.
30. Federsel, C.; Ziebart, C.; Jackstell, R.; Baumann, W.; Beller, M., Catalytic Hydrogenation of Carbon Dioxide and Bicarbonates with a Well-Defined Cobalt Dihydrogen Complex. *Chem. Eur. J.* **2012,** *18*, 72-75.
31. Burgess, S. A.; Kendall, A. J.; Tyler, D. R.; Linehan, J. C.; Appel, A. M., Hydrogenation of CO2 in Water Using a Bis(diphosphine) Ni–H Complex. *ACS Catal.* **2017,** *7*, 3089-3096.
32. Zall, C.; Linehan, J.; Appel, A., A Molecular Copper Catalyst for Hydrogenation of CO2 to Formate. *ACS Catal.* **2015,** *5*, 150805132443001.
33. Trivedi, M.; Kumar, A.; Husain, A.; Rath, N. P., Copper(I) Complexes Containing PCP Ligand Catalyzed Hydrogenation of Carbon Dioxide to Formate under Ambient Conditions. *Inorg. Chem.* **2021,** *60*, 4385-4396.
34. Boudreaux, C. M.; Nugegoda, D.; Yao, W.; N., L.; Frey, N. C.; Li, Q.; Qu, F.; Zeller, M.; Webster, E.; Delcamp, J. H.; Papish, E. T., Low Valent Cobalt(I) CNC Pincer Complexes as Catalysts for Light Driven Carbon Dioxide Reduction. *ACS Catal.* **2022,** *12*, 8718-8728.
35. Burks, D. B.; Davis, S.; Lamb, R. W.; Liu, X.; Rodrigues, R. R.; Liyanage, N. P.; Sun, Y.; Webster, C. E.; Delcamp, J. H.; Papish, E. T., Nickel(II) pincer complexes demonstrate that the remote substituent controls catalytic carbon dioxide reduction. *Chem. Commun.* **2018,** *54*, 3819-3822.
36. Manafe, S. Y.; Le, N.; Lambert, E. C.; Curiac, C.; Nugegoda, D.; Das, S.; Hunt, L. A.; Qu, F.; Whitt, L. M.; Fedin, I.; Hammer, N. I.; Webster, C. E.; Delcamp, J. H.; Papish, E. T., Sensitized and Self-Sensitized Photocatalytic CO2 Reduction to HCO2– and CO under Visible Light with Ni(II) CNC-Pincer Catalysts. *ACS Catal.* **2024**, 6589-6602.
37. Yao, W.; Das, S.; DeLucia, N. A.; Qu, F.; Boudreaux, C. M.; Vannucci, A. K.; Papish, E. T., Determining the Catalyst Properties That Lead to High Activity and Selectivity for Catalytic Hydrodeoxygenation with Ruthenium Pincer Complexes. *Organometallics* **2020,** *39*, 662-669.

38. Das, S.; Nugegoda, D.; Qu, F.; Boudreaux, C. M.; Burrow, P. E.; Figgins, M. T.; Lamb, R. W.; Webster, C. E.; Delcamp, J. H.; Papish, E. T., Structure Function Relationships in Ruthenium Carbon Dioxide Reduction Catalysts with CNC Pincers Containing Donor Groups. *Eur. J. Inorg. Chem.* **2020,** *2020*, 2709-2717.
39. Mika, L. T.; Tuba, R.; Tóth, I.; Pitter, S.; Horváth, I. T., Molecular Mapping of the Catalytic Cycle of the Cobalt-Catalyzed Hydromethoxycarbonylation of 1,3-Butadiene in the Presence of Pyridine in Methanol. *Organometallics* **2011,** *30*, 4751-4764.
40. Hollingsworth, R. L.; Beattie, J. W.; Grass, A.; Martin, P. D.; Groysman, S.; Lord, R. L., Reactions of dicobalt octacarbonyl with dinucleating and mononucleating bis(imino)pyridine ligands. *Dalton Trans.* **2018,** *47*, 15353-15363.
41. Addison, A. W.; Rao, T. N.; Reedijk, J.; Rijn, J. v.; Verschoor, G. C., Synthesis, structure, and spectroscopic properties of copper(II) compounds containing nitrogen–sulphur donor ligands; the crystal and molecular structure of aqua[1,7-bis(N-methylbenzimidazol-2-yl)-2,6-dithiaheptane]copper(II) perchlorate. *J. Chem. Soc., Dalton Trans.* **1984**, 1349 - 1356.
42. Das, S.; Rodrigues, R. R.; Lamb, R. W.; Qu, F.; Reinheimer, E.; Boudreaux, C. M.; Webster, C. E.; Delcamp, J. H.; Papish, E. T., Highly Active Ruthenium CNC Pincer Photocatalysts for Visible-Light-Driven Carbon Dioxide Reduction. *Inorg. Chem.* **2019,** *58*, 8012-8020.
43. Boudreaux, C. M.; Liyanage, N. P.; Shirley, H.; Siek, S.; Gerlach, D. L.; Qu, F.; Delcamp, J. H.; Papish, E. T., Ruthenium(II) complexes of pyridinol and N-heterocyclic carbene derived pincers as robust catalysts for selective carbon dioxide reduction. *Chem. Commun.* **2017,** *53*, 11217-11220.
44. Pérez, E. R.; da Silva, M. O.; Costa, V. C.; Rodrigues-Filho, U. P.; Franco, D. W., Efficient and clean synthesis of N-alkyl carbamates by transcarboxylation and O-alkylation coupled reactions using a DBU–CO2 zwitterionic carbamic complex in aprotic polar media. *Tetrahedron Letters* **2002,** *43*, 4091-4093.
45. Heldebrant, D. J.; Jessop, P. G.; Thomas, C. A.; Eckert, C. A.; Liotta, C. L., The Reaction of 1,8-Diazabicyclo[5.4.0]undec-7-ene (DBU) with Carbon Dioxide. *The Journal of Organic Chemistry* **2005,** *70*, 5335-5338.
46. Bielinski, E. A.; Förster, M.; Zhang, Y.; Bernskoetter, W. H.; Hazari, N.; Holthausen, M. C., Base-Free Methanol Dehydrogenation Using a Pincer-Supported Iron Compound and Lewis Acid Co-catalyst. *ACS Catal.* **2015,** *5*, 2404-2415.